Title

Coupled baryon diffusion and nucleosynthesis in the early universe

Journal

The Astrophysical Journal, 358(1)

ISSN

0004-637X

Authors

Mathews, GJ
Meyer, BS
Alcock, CR
et al.

Publication Date

1990-07-01

DOI

10.1086/168961

Peer reviewed

THE ASTROPHYSICAL JOURNAL, 358:36–46, 1990 July 20

COUPLED BARYON DIFFUSION AND NUCLEOSYNTHESIS IN THE EARLY UNIVERSE

G. J. MATHEWS, B. S. MEYER, AND C. R. ALCOCK
Institute of Geophysics and Planetary Physics, Lawrence Livermore National Laboratory
AND
G. M. FULLER
Physics Department, University of California, San Diego
Received 1989 November 17; accepted 1990 January 24

ABSTRACT

We report on calculations of primordial nucleosynthesis in baryon-number inhomogeneous big bang models. Nucleosynthesis yields are presented as a function of Ω_b for a range of parameters which characterize the amplitude, shape, and mean separation of isothermal baryon-number fluctuations assumed to arise from an earlier epoch. We follow the modification of these fluctuations due to neutron and proton diffusion before, during, and after nucleosynthesis, using a multizone computer code which couples the diffusion equation with the nuclear reaction network and the universal expansion. The resulting abundance yields are strongly dependent upon the parameters characterizing the fluctuations; however, there exists a range of these parameters in which the calculated light-element abundances are in agreement with observational constraints for considerably higher values of Ω_b than that allowed by the standard homogeneous big bang.

Subject headings: abundances — early universe — elementary particles — nucleosynthesis

I. INTRODUCTION

Recent work (Applegate, Hogan, and Scherrer 1987, 1988; Alcock, Fuller, and Mathews 1987; Fuller, Mathews, and Alcock 1988; Malaney and Fowler 1988; Audouze *et al.* 1988; Terasawa and Sato 1989; Kurki-Suonio *et al.* 1988, 1990; Kurki-Suonio and Matzner 1989) has shown that if isothermal baryon-number fluctuations (hereafter simply referred to as fluctuations) are created in an epoch of the early universe prior to nucleosynthesis, then the primordial nucleosynthetic abundance yields could differ significantly from those of the standard homogeneous big bang. Although the emphasis in most of the above works has been on models in which the universe is closed by baryons, there can be significant effects for any fraction of the closure density contributed by baryons.

It is important to keep in mind, however, that the light-element abundance yields in these inhomogeneous models depend upon a number of uncertain features of the calculations. These features include the amplitude, shape, and spatial distribution of the fluctuations, as well as fluctuation modification by baryon diffusion and possible hydrodynamic processes, before and during the nucleosynthesis epoch (Fuller, Mathews, and Alcock 1989; Mathews *et al.* 1989; Applegate, Hogan, and Scherrer 1988; Alcock *et al.* 1990). Furthermore, the nuclear reactions and baryon diffusion must be evolved simultaneously because the time scale for baryon diffusion is comparable to the time scale for many of the relevant nuclear reactions during primordial nucleosynthesis. In this paper we therefore attempt to gain a better perspective on the nucleosynthesis yields derived from inhomogeneous big bang models by making a study of abundance yields for a broad range of characteristic fluctuation amplitudes, shapes, and separation distances. We use a multizone model which solves the baryon diffusion and nucleosynthesis implicitly. This is a substantial improvement over a number of previous studies which utilized simple schematic treatments of the effects of baryon diffusion (Applegate, Hogan, and Scherrer 1987, 1988; Alcock, Fuller, and Mathews 1987; Fuller, Mathews, and Alcock 1988, 1989; Malaney and Fowler 1988). Our approach is similar to that of Kurki-Suonio and Matzner (1989, hereafter KM89). However, our calculation is based upon an independently developed computer code which implicitly solves the diffusion and nucleosynthesis equations simultaneously and therefore provides an important check on the results of KM89. We also consider a broader range of fluctuation characteristics than in KM89. This extended parameter range includes larger fluctuation amplitudes and different fluctuation shapes.

We utilize a parameterization of the basic characteristics of isothermal baryon-number fluctuations which is motivated and described in § II. In § III we discuss details of the multizone primordial nucleosynthesis code in which the nuclear reaction network and the baryon diffusion equations are solved implicity as the universe expands. Results are presented in § IV for a range of closure densities, Ω_b, and fluctuation characteristics. We find, as in KM89 and Kurki-Suonio *et al.* (1990), that when the diffusion and nucleosynthesis are carefully followed, it is more difficult to satisfy the light-element abundance constraints for a universe with $\Omega_b = 1$ than in the simpler schematic models, even in our expanded parameter space. Nevertheless, significantly higher values of Ω_b are allowed in such inhomogeneous models than in the standard homogeneous big bang or inhomogeneous models with a more restricted range of fluctuation characteristics (Terasawa and Sato 1989; Kurki-Suonio *et al.* 1990).

In two forthcoming papers (Alcock *et al.* 1990; Meyer *et al.* 1990) we will extend this work to consider two additional effects which may also alter the primordial light-element abundance yields: the hydrodynamic modification of the fluctuations which is likely to occur near the end of nucleosynthesis; and the effect of averaging over a distribution of fluctuation separation distances rather than assuming a regular lattice structure as is done here. The present work serves to elucidate the interesting regions of parameter space for such subsequent work.

II. CHARACTERIZATION OF THE FLUCTUATIONS

Significant modification of the primordial nucleosynthesis yields relative to those of the standard homogeneous big bang can occur as long as the separation between fluctuations is larger than the proton diffusion length before the epoch of nucleosynthesis. Though one might imagine any number of processes that could produce such baryon-density fluctuations, i.e., decay of strangelets (Alcock and Farhi 1985), evaporating soliton stars (Lee 1987), or superconducting cosmic strings (Malaney and Butler 1989), a first-order QCD phase transition is most often proposed (Witten 1984; Applegate and Hogan 1985) and will be discussed here in the context of determining reasonable parameters to characterize the fluctuations.

In our previous papers we presented simple ideal gas models of a deconfined quark-gluon plasma and of a confined hadron gas (Alcock, Fuller, and Mathews 1987; Fuller, Mathews, and Alcock 1988, 1989). These models were used to identify the relevant strong interaction physics and served as a basis for estimating the amplitude, shape, and distribution of baryon density fluctuations which might have emerged from a QCD phase transition. At the present time, however, it appears that further progress in quantifying the characteristic parameters of the fluctuations will be limited until more detailed models of the QCD physics become available.

For the present purposes, we therefore parameterize those physical quantities which are likely to have the most important consequences for primordial nucleosynthesis. However, we emphasize that this is only a crude parameterization of possible fluctuation characteristics to emerge from a cosmic QCD phase transition or any other phenomenon which might produce baryon-number inhomogeneities. There is probably a much broader parameter space yet to be explored, and this work should only be viewed as a sampling from that space.

Although we will follow the baryon diffusion and nucleosynthesis in many zones, it is convenient to characterize the initial fluctuations (at $T = 100$ MeV) by regions with two different baryon densities separated by a sharp boundary. The choice of a sharp boundary is not unreasonable because baryon diffusion will remove the initial discontinuity before the onset of primordial nucleosynthesis. For this choice of fluctuation shape, the quantities which characterize the fluctuation are the ratio of baryon number densities, R, the mean separation between nucleation sites, l, the volume fraction, f_v, occupied by the high-density zones, and the total baryonic contribution to the closure density, Ω_b. This latter quantity we relate to the baryon-to-photon ratio by assuming a Hubble constant of $H_0 = 50$ km s^{-1} Mpc^{-1} and a present background temperature of 2.7 K.

When the baryon chemical potential is much less than the temperature (which is the case for the early universe), the equilibrium ratio of baryon densities is also equal to the instantaneous ratio of baryon number susceptibilities, R_I, a quantity which can in principle be extracted from Monte-Carlo lattice QCD calculations (Gottlieb *et al.* 1987). The ratio of susceptibilities is:

$$R_I \equiv [\partial^2\Omega_Q/\partial\mu^2)_{T,V}]/[(\partial^2\Omega_H/\partial\mu^2)_{T,V}] , \quad (1)$$

where Ω_Q is the thermodynamic potential for the quark-gluon plasma phase, and Ω_H is the thermodynamic potential for the chiraly-broken, or confined, hadron phase (Fuller, Mathews, and Alcock 1988).

The ideal gas models suggest that $R_I \cong 100$ (Alcock, Fuller, and Mathews 1987). Recent lattice calculations (Gottieb *et al.* 1987) indicate that the ideal gas model gives a reasonable estimate of $(\partial^2\Omega_Q/\partial\mu^2)$; however, the lattice calculations give no good estimate of $(\partial^2\Omega_H/\partial\mu^2)$, except that it is sufficiently small to ensure that $R_I \geq 10$ (Gottlieb *et al.* 1987).

The amplitude and shape of the fluctuations depend upon R_I in a complicated and as yet poorly understood manner. As the phase boundary moves during the transition, baryon number tends to be concentrated. The larger R_I is, the larger will be the eventual amplitude of the fluctuation. The degree of concentration of baryon number and, hence, the ultimate amplitude and shape of the fluctuation also depend upon the baryon number transport processes both away from and across the phase boundaries (Fuller, Mathews, and Alcock 1988, 1989; Kurki-Suonio 1988).

The rate of baryon number transport across the phase boundaries (i.e., the baryon transmission probability) is not known but has been studied in the context of a chromoelectric flux-tube model (Sumiyoshi *et al.* 1989) and related to the fluctuation characteristics (Fuller, Mathews, and Alcock 1988). During the phase transition, baryon-number transport away from the walls is sensitive to fluid velocities induced by the expansion of the universe, gravitational interactions among the fluctuations, and by the possible effects of turbulence (Fuller, Mathews, and Alcock 1989; and Alcock *et al.* 1989). In the extreme limit where transport away from the walls is taken to occur only via microscopic diffusion, which is inefficient, the eventual fluctuation amplitudes are only of the order of R_I (Kurki-Suonio 1988). However, the baryon-number transport may be augmented by eddy-current mixing that will lead to amplitudes which are much larger than R_I (Fuller, Mathews, and Alcock 1989). We will consider such baryon number transport processes in more detail in a forthcoming paper. For the present work, however, we feel justified in considering a larger range of fluctuation amplitudes than in KM89. We parameterize the fluctuation amplitude at the end of the phase transition by the ratio, R, of the baryon number density in the highest density zone to that in the lowest density zone.

In this work we assume that the fluctuations are arranged in a regular lattice. If the separation between the centers of the fluctuations is l, then one can imagine each fluctuation site to be contained within a sphere of radius $r = l/2$. Space is then filled by a body-centered cubic lattice of spherical cells. Each cell is initially divided into a number of zones at high density and an equal number at low density. For the best numerical accuracy, we can take the zoning to be finest at the boundary between the high- and low-density zones and somewhat coarser away from the boundary as illustrated in Figure 1. We have computed results using up to 32 zones; however, we find that good numerical accuracy can be maintained with only eight or 16 zones, depending upon the fluctuation amplitude.

Figure 2 shows an example of the convergence of these calculations as the number of zones is increased. Plotted is the calculated ^{4}He mass fraction, Y_p, as a function of separation distance for an $\Omega_b = 1.0$, $R = 10^6$, $f_v^{1/3} = 0.25$ spherical fluctuation with eight, 16, and 32 zones. The eight-zone run has the partitioning shown in Figure 1. The 16-zone run further divides up zones four and five of the eight-zone run to give much finer zoning at the boundary of the high- and low-density regions. For the 16-zone run in Figure 2, the smallest zone has a width of 1/152 of the radius of the whole cell. For the 32-zone run, each of the zones of the 16-zone run were halved. We also ran a 32-zone case in which zones eight and

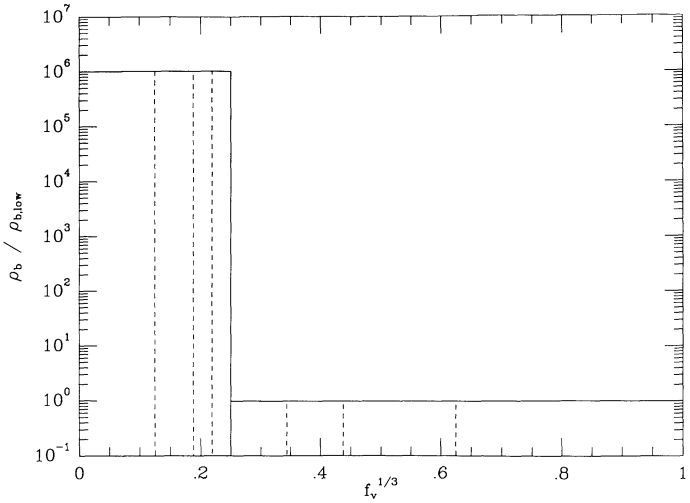

FIG. 1.—An example of the variable zoning in our calculations. For best numerical accuracy, the zoning is finest near the boundary between the high- and low-density regions.

nine of the 16-zone run were further divided up. In this case, the smallest zone had a width of 1/131,072 of the total radius. The results for these latter runs were essentially identical with those of the 16-zone run. Significant differences exist, however, between the eight- and 16-zone runs.

At large fluctuation radii, too coarse zoning at the boundary of the high- and low-density regions leads to an underestimate of the diffusion of neutrons out of the high-density region because the effective numerical gradients are smaller. At small fluctuation radii, coarse zoning also leads to an overestimate of diffusion back into the high-density region after nucleosynthesis has begun, because the diffusion length for a neutron in the high-density zones may be much less than the zone width. These combined effects lead to errors in the solution to the diffusion equation and account for why in our earlier preliminary reports on baryon coupled diffusion, which utilized only eight zones (Mathews *et al.* 1989; Kajino, Mathews, and Fuller 1989), the helium yields were lower than those reported here for models with large fluctuation amplitude. No significant differences exist between the 16- and 32-zone runs. We have found this to be true for all fluctuation parameters studied, and consequently, we use 16-zone runs in all our calculations.

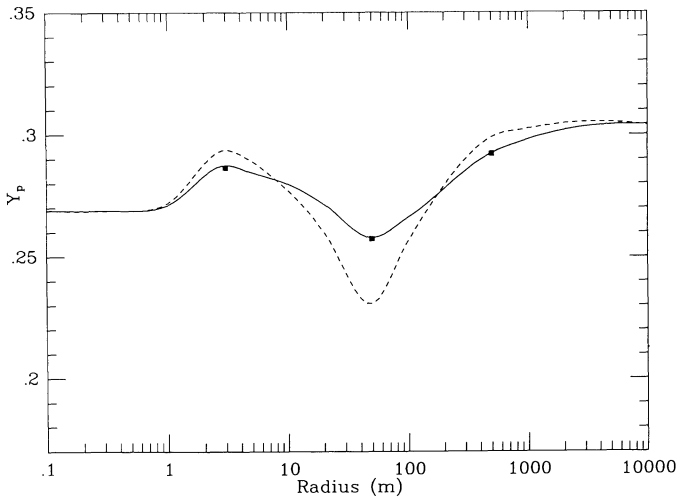

FIG. 2.—An illustration of the convergence of the numerical results as the number of zones is increased in the calculation. Shown is the helium mass fraction as a function of separation radius from calculations using eight zones (*dashed line*), 16 zones (*solid line*), and 32 zones (*square points*).

We consider two geometries for the cells: in one, the high-density zones are at the center (i.e., condensed spheres); in the other, the high-density zones are at the outer edge (i.e., spherical shells). These two shapes probably do not bracket all possible geometries for such fluctuations. For example, we do not consider the planar fluctuations studied in KM89. However, these two shapes should approximate two possible extreme consequences of a first-order QCD phase transition; i.e., the spheres may result when the surface tension of the regions of quark-gluon plasma is large, and spherical shells may approximate the geometry resulting from low bubble surface tension (Fuller, Mathews, and Alcock 1988).

In our previous work (Alcock, Fuller, and Mathews 1987; Fuller, Mathews, and Alcock 1988) we employed classical nucleation theory to estimate l, the mean separation between the centers of the cells at the end of the phase transition. It was found in that work that l depended parametrically upon the surface tension, σ, between the two phases. The value of σ cannot be reliably estimated in current strong interaction models, though there are a few attempts to calculate σ in lattice QCD (Frei and Patkos 1989; Toussaint 1989). For the present purposes, we will take l as a free parameter in the range found in our previous work, $0.1\ m \leq l/2 \leq 10$ km at $T = 100$ MeV which corresponds to a range of 1.3 to 1.3×10^4 km at 100 keV when nucleosynthesis begins. We note here that our analysis of the connection between l and σ in Fuller, Mathews, and Alcock (1988) contained a numerical error which, given the uncertainty in σ and the temperature of the phase transition, does not effect our estimate of the appropriate range of l (see Meyer *et al.* 1989).

III. PRIMORDIAL NUCLEOSYNTHESIS AND BARYON DIFFUSION

The earliest treatments (Applegate, Hogan, and Scherrer 1987; Alcock, Fuller, and Mathews 1987; Fuller, Mathews, and Alcock 1988; Audouze *et al.* 1988) of primordial nucleosynthesis in a universe with isothermal baryon number inhomogenities involved a schematic model in which the neutron density was taken to be homogeneous just before nucleosynthesis. Any further effects of baryon diffusion were neglected. This was a convenient simplification for the purposes of a global parameter study. However, it has been pointed out (Malaney and Fowler 1988; Mathews *et al.* 1989; KM89; Terasawa and Sato 1989) that baryon diffusion both prior to and after the onset of primordial nucleosynthesis can significantly influence the calculated final light-element abundances.

It is thus necessary to solve simultaneously the baryon diffusion equation and nuclear reaction rates during the period from immediately after the phase transition to the end of nucleosynthesis. We do this by noting that the rate of change of the proper number density, n_i, of a given species, i, can be written:

$$\partial n_i/\partial t = (\text{production rates}) - (\text{destruction rates}) - 3Hn_i + \nabla(D_i \nabla n_i)\,, \quad (2)$$

where the production and destruction terms represent nuclear

reaction rates. H is the Hubble expansion parameter, and D_i is the microscopic diffusion coefficient. In this paper, we take D_i to be zero except for neutrons and protons. Although it is technically incorrect to ignore the diffusion of the other charged species, the diffusion constants for heavier species are smaller than the proton diffusion constant due to their higher charges and masses. The total neutron diffusion coefficient is

$$D_n^{-1} = D_{ne}^{-1} = D_{np}^{-1} , \quad (3)$$

where the proper diffusion coefficients for neutron-electron scattering, D_{ne}, and neutron-proton scattering, D_{np}, are taken from Applegate, Hogan, and Scherrer (1987) correcting for a minor arithmetic error in the numerical coefficient for D_{ne} given in that paper. Similarly, the proton diffusion coefficient is

$$D_p^{-1} = D_{pe}^{-1} + D_{pn}^{-1} , \quad (4)$$

where D_{pe}, the coefficient for proton-electron scattering, is again taken from Applegate, Hogan, and Scherrer (1987). D_{pn} is the coefficient for the scattering of protons from neutrons. This quantity is related to D_{np} by

$$D_{pn} = (X_n/X_p)D_{np} , \quad (5)$$

where X_n and X_p are the local neutron and proton mass fractions, respectively. This last equation corrects D_{np} for the fact that the roles of the neutrons and protons are interchanged in the scattering leading to proton diffusion.

We approximate flux-limited diffusion by fixing a maximum value of the diffusion coefficient for each species. This avoids a breakdown of the diffusion approximation when the mean free path of a species against scattering becomes too great. If r is the radius of a cell, and v_i is an average thermal velocity for a given species i, then we take

$$D_i \leq rv_i . \quad (6)$$

We have found that it is imperative to solve the simultaneous set of equation (2) implicity, since the time step of the calculation can be set by either the nuclear reaction rates or the baryon diffusion rates. This differs from KM89, who solved the nucleosynthesis and diffusion equations separately. The finite differenced version of equation (2) is a nearly block-diagonal matrix whose submatrices are connected via the diffusion matrix elements. Our present computer code follows the evolution of nuclear abundances in up to 32 zones of variable spacing in radius from $T = 10^{12}$ K to the end of nucleosynthesis, typically $T = 10^6$ K.

As mentioned above, we have chosen to consider two-part spherical fluctuations. The inner part has an outer radius that is a fraction, $f_v^{1/3}$, of the total fluctuation radius. The density ratio of the high-density to low-density regions of the fluctuation is R. We have performed a series of calculations with a range of parameters, and we compare those results with primordial abundance constraints. We choose $R = 10^2$, 10^3, 10^4, and 10^6 and $f_v^{1/3} = 0.0625$, 0.125, 0.25, and 0.5 for the high-density region. We found that there was little change in the results when going to yet larger fluctuation amplitudes, although it was necessary to include many more zones to guarantee convergence. Furthermore, on the mass scales considered here fluctuations as large as $R = 10^6$ or more may be damped by neutrino diffusion (Applegate and Hogan 1985). For all calculations, we use three neutrino species and a 10.35-minute neutron half-life. There is some recent evidence that the neutron half-life could be as low as 10.25 ± 0.04 (Mampe *et al.* 1989). This could reduce our calculation of Y_p by $\sim 0.2\%$.

IV. RESULTS

Figure 3 shows the calculated primordial helium mass fraction, Y_p, for an $\Omega_b = 1.0$ inhomogeneous universe as a function of fluctuation cell radius, $r = l/2$ (at $T = 100$ MeV), fluctuation amplitude R, and cell volume fraction, $f_v^{1/3}$. Results for both "spherically condensed" and "shell" fluctuations are shown. Figure 4 shows the same curves for an $\Omega_b = 0.1$ inhomogeneous universe. Since the ^{4}He abundance in these inhomogeneous big bang models is less likely to be modified by hydrodynamic effects during nucleosynthesis (Alcock *et al.* 1989) or by subsequent galactic chemical evolution effects (Dearborn *et al.* 1989; Mathews, Alcock, and Fuller 1990) than the abundances of ^{2}H and ^{7}Li, it is potentially the most important diagnostic of early universe characteristics. Figures 5 and 6 show results for the abundances of ^{2}H, ^{3}He, and ^{7}Li relative to hydrogen for $\Omega_b = 1.0$ and 0.1, respectively. We note that for $R = 100$, our calculations overlap with the condensed-sphere calculations of KM89 for $f_v = \frac{1}{8}$ and $\frac{1}{4}$. There is overall very good agreement between KM89 and our results for the abundances of ^{2}H, ^{3}He, ^{4}He, and ^{7}Li over the whole range of fluctuation separation (cell radius) considered.

For $Rf_v \geq 1.5$ and $r = 30$–200 m (spheres) or $f_v^{1/3} < 0.125$ and $r = 200$–600 m (shells), a minimum in the ^{4}He and ^{7}Li abundances and a sharp increase in the ^{2}H abundance emerge. The occurrence of this minimum for ^{4}He and ^{7}Li and the increase in ^{2}H may allow for the observed abundance constraints to be satisfied in a universe with much higher values of Ω_b than that allowed by the standard homogeneous big bang. Therefore, it is crucial to understand this phenomenon.

Consider first the ^{4}He abundance curves (Figs. 3 and 4). In standard big bang nucleosynthesis, the ^{4}He mass fraction is given to a good approximation by twice the neutron mass fraction just before the beginning of nucleosynthesis (at $T \sim 10^9$ K). In inhomogeneous big bang models, most of the total ^{4}He abundance is produced in high-density regions. Therefore, the presence of the minimum in the curve of ^{4}He abundance versus cell radius, r, results from an optimization of the effects of diffusion and nuclear reactions which removes neutrons from the high-density regions and increases the neutron density in the low-density regions. Basically, there are two effects to consider. When the fluctuations are close together, the time scale for neutron diffusion is short compared to the expansion time scale. Therefore, neutrons can easily diffuse out of the high-density regions. However, if the fluctuations are too close together, the neutrons will also quickly diffuse back into the high-density regions as they are depleted in those zones by nuclear reactions (Malaney and Fowler 1988). If this process is too efficient, it will result in increased ^{4}He production (and decreased ^{2}H) even relative to the standard $\Omega_b = 1.0$ big bang, because nucleosynthesis is occurring mostly in regions with local $\Omega_b > \langle\Omega_b\rangle_{\rm avg}$. This is the reason for the shoulder to the left of the Y_p minimum in Figures 3 and 4. On the other hand, if the fluctuations are too far apart, the proper distances become large compared to the diffusion distance during the epoch of nucleosynthesis. Hence, little diffusion of neutrons out of the high-density zones occurs before the end of nucleosynthesis, and the results asymptotically approach those of two separate standard big-bang models with different values for Ω_b.

The ^{4}He minima in Figures 3 and 4 correspond to condi-

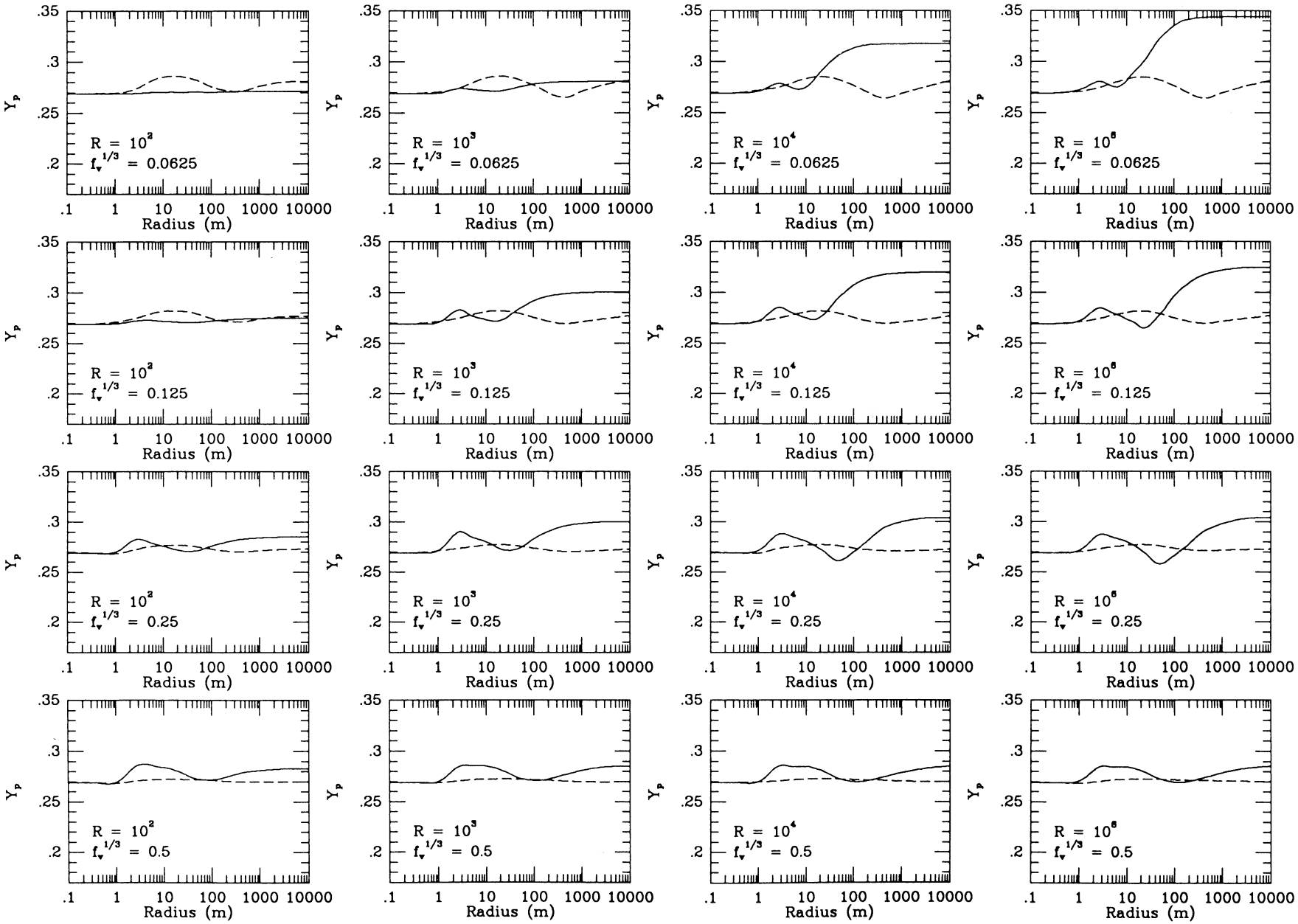

FIG. 3.—Calculated helium mass fraction from $\Omega_b = 1.0$ inhomogeneous nucleosynthesis models. Results are plotted as a function of separation radius, for different values of the fluctuation amplitude, R, and fluctuation fractional radius, $f_v^{1/3}$. Solid lines are for the condensed-sphere geometry. Dashed lines are for spherical shells.

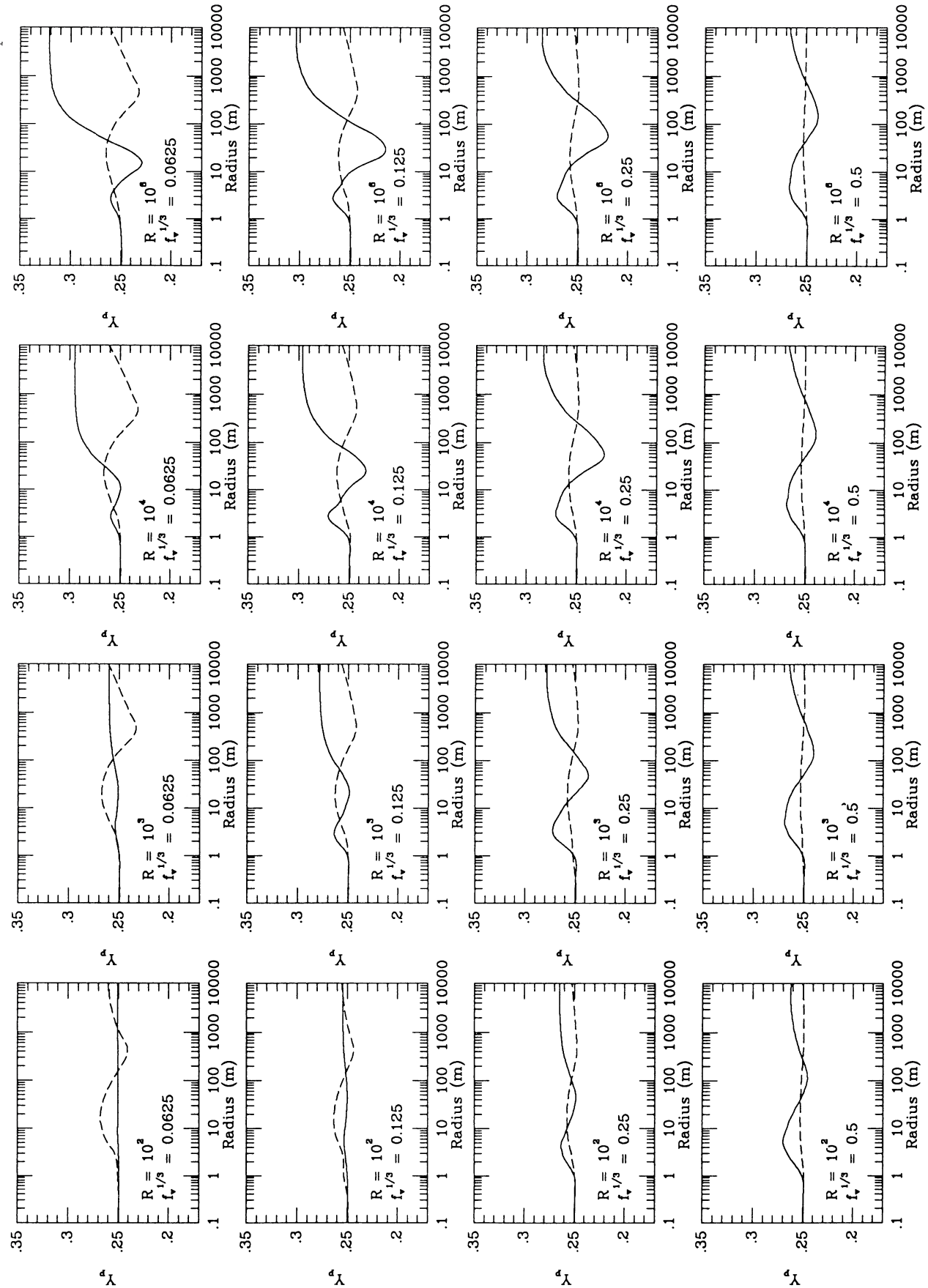

FIG. 4.—Same as Fig. 2, but for $\Omega_b = 0.1$

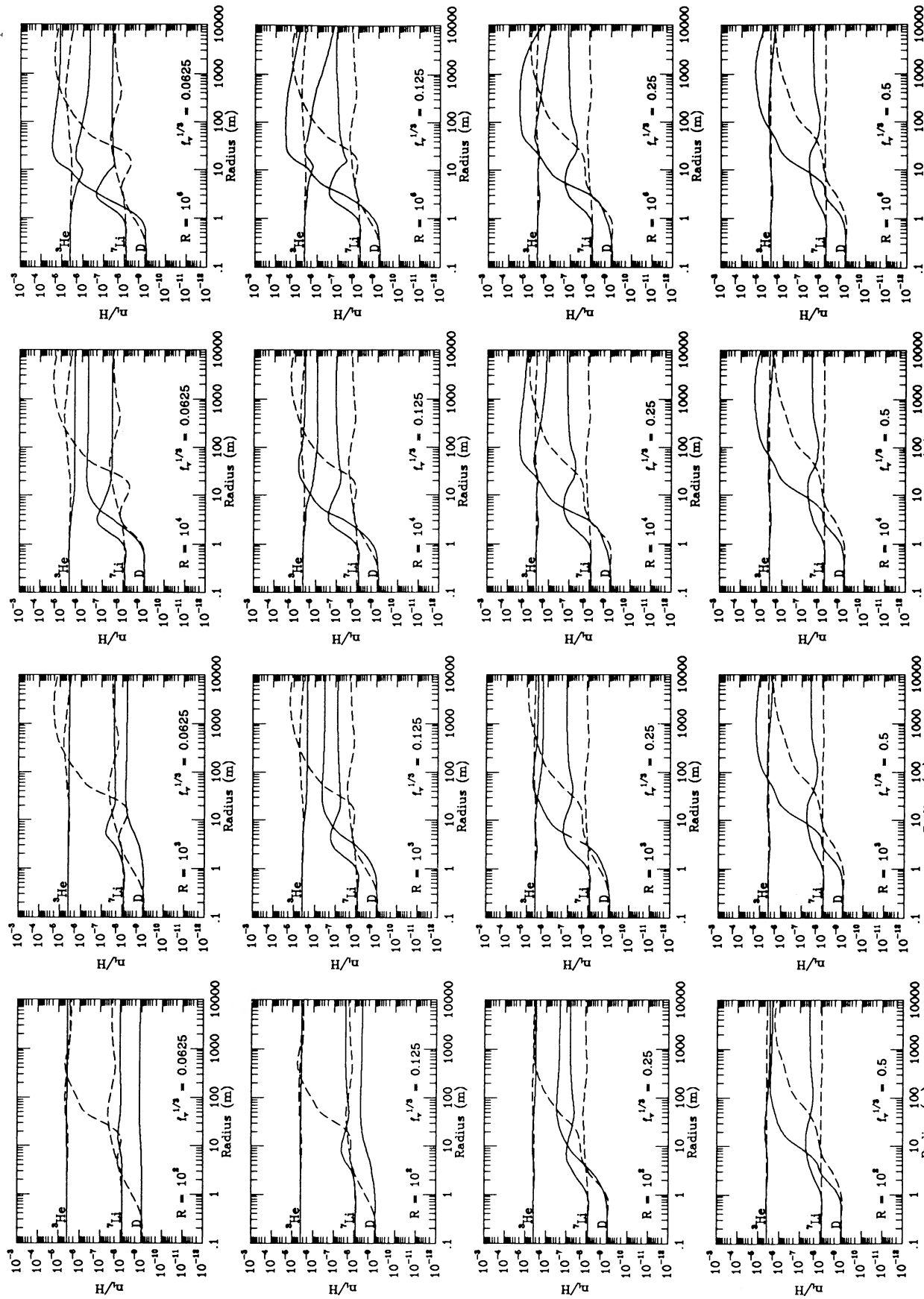

FIG. 5.—Calculated light-element abundances relative to hydrogen from $\Omega_b = 0.1$ inhomogeneous nucleosynthesis models. Results are plotted as a function of separation radius, r, for different values of the fluctuation amplitude, R, and fluctuation radius fraction, $f_v^{1/3}$. Solid lines are for the condensed sphere geometry, and dashed lines are for spherical shells.

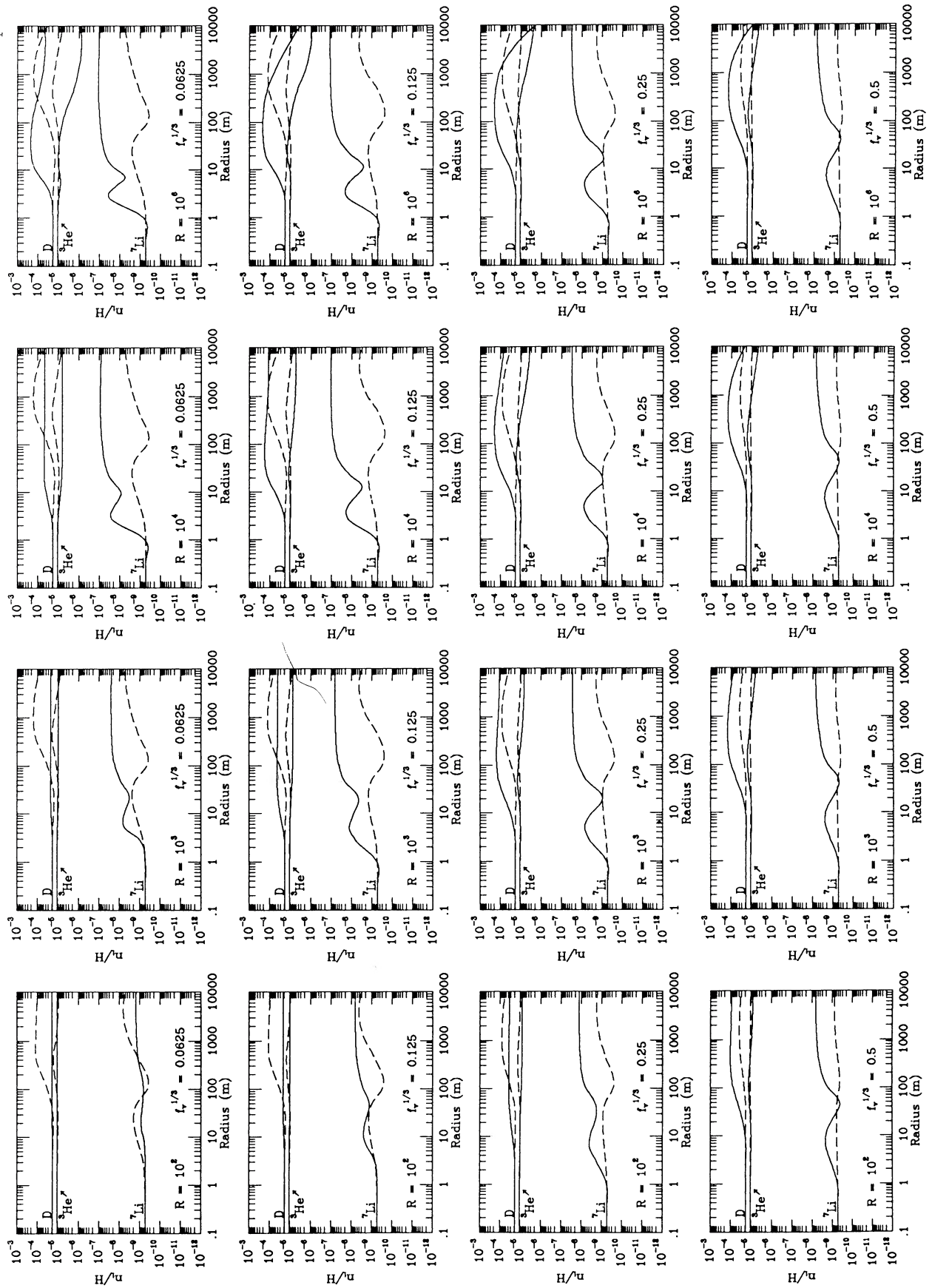

FIG. 6.—Same as Fig. 4, but for $\Omega_b = 0.1$

tions in which there is both substantial diffusion of neutrons prior to nucleosynthesis and a sufficient separation between fluctuations that the diffusion of neutrons back into the high-density zones after nucleosynthesis is inhibited. The back diffusion into the high-density zones is limited by both the increased proper distance for the neutrons to travel (due to universal expansion) and (for R sufficiently large) the shorter mean free path for neutrons in the high-density zones.

The features in the other light-element abundances (Figs. 5 and 6) have a similar interpretation to the minimum in the helium mass fraction. For $r \geq 10$ m, an increase in the ^{2}H abundance results from the diffusion of neutrons into the low-density zones where ^{2}H is made. For $r \leq 1$ m, there is no difference between the standard big bang and inhomogeneous big bang results for any of the light-element abundances including ^{4}He, because there is sufficient diffusion of both protons and neutrons before nucleosynthesis to eliminate the fluctuations. For ^{7}Li, there is the added effect from increased ^{7}Be destruction by the ^{7}Be$(n,p)^7$Li$(p,\alpha)^4$He reaction caused by neutron diffusion back into the high-density regions at late times (Malaney and Fowler 1988). Since this backflow effect is optimized for smaller separations, the minimum in the ^{7}Li abundance curve tends to occur for separation distances slightly less than that for ^{4}He.

Figure 7 illustrates the time history of the comoving neutron density for an optimum spherical fluctuation configuration with $\Omega_b = 1.0$, $R = 10^6$, $f_v^{1/3} = 0.25$, and $r = 50$ m. Up to $t \sim 10$ s, there is significant diffusion of neutrons into the low-density zones. This is evidenced by the increased neutron density in the low-density zones by as much as four orders of magnitude and the decreased neutron density for the high-density zones by as much as an order of magnitude. This diffusion eventually leads to decreased ^{4}He production in the high-density regions and enhanced ^{2}H production in the low-density regions. The low-density zones come into neutron-diffusion equilibrium by $t \sim 50$ s, which is about the time that nucleosynthesis begins in the innermost high-density zone. By $t = 100$ s, the loss of neutrons by nuclear reactions in the high-density regions causes the neutron density in all the zones to be nearly equal. However, further nuclear reactions will then continue to deplete neutrons from the high-density zones by as much as eighteen orders of magnitude. At this point, neutrons begin to diffuse back into the high-density regions (Malaney and Fowler 1988). Between $t \sim 200$–1000 s, the back diffusion of neutrons is roughly cancelled by the neutron capture reactions and the neutron density in the different zones changes. Between 1000 and 2000 s, a neutron diffusion equilibrium is obtained in all zones. Beyond 2000 s, most of the original big bang neutrons would have decayed. However, some neutrons remain due to production of neutrons, primarily by the D$(D, n)^3$He reaction.

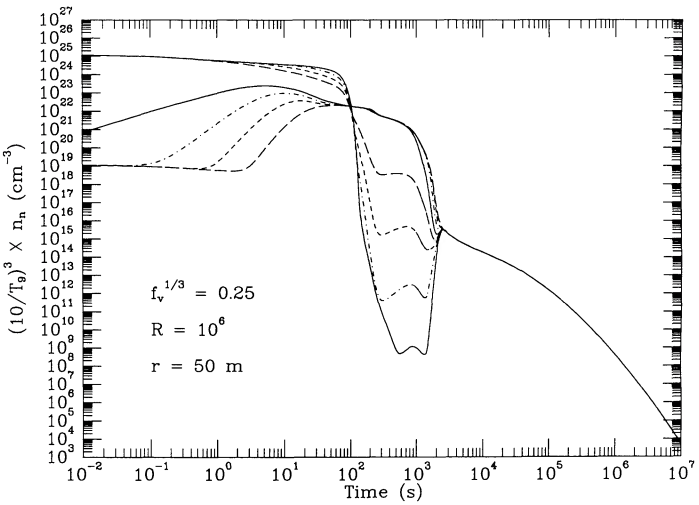

FIG. 7.—Comoving neutron density as a function of time for eight different zones in a calculation with $R = 10^6$, $f_v^{1/3} = 0.25$, $r = 50$ m, and $\Omega_b = 1.0$. Solid line corresponds to the innermost zones in the high- and low-density regions. Long dashed lines are for the outermost zones in each region.

Additional insight can be obtained from Figure 8, which shows the nucleosynthetic yields, $\Omega_i X_i \Delta f_v / \Delta f_v^{1/3}$, as a function of $f_v^{1/3}$, for the different light-element species in the same run with $\Omega_b = 1.0$, $f_v^{1/3} = 0.25$, $R = 10^6$, and $r = 50$ m. The integral of these histograms over $f_v^{1/3}$ will directly give the average mass fraction. These histograms, therefore, display the relative contribution to the final average abundances of each zone. From this figure, one can see that most of the helium is produced in the high-density zones, with a large contribution arising in a spike at the boundary between the low- and high-density regions. This large contribution at the boundary is caused by the combination of high baryon density and high neutron mass fraction as the neutrons diffuse out of or into the high-density regions. A similar effect is observed for D and ^{3}He. For D, one can also clearly see that the dominant contribution is in the low-density zones. For ^{3}He, most of the nucleosynthesis is as ^{3}He in the high-density zones and at the boundary. For ^{7}Li, one can see that most of the nucleosynthesis occurs in the high–baryon-density regions by the ^{3}He$(\alpha,\gamma)^7$Be reaction. There is also an important depletion of ^{7}Li at the boundary due to the flow of neutrons from the low-density zones (after neutrons are exhausted in the high-density regions). The depletion is caused by the ^{7}Be$(n,p)^7$Li$(p,\alpha)^4$He reactions (Malaney and Fowler 1988). It is worth noting that the magnitude of this depletion is less than that speculated in Malaney and Fowler (1988) due to the short mean free path of the neutrons in the high-density regions which prohibits their penetration into the high-density zones.

The results from the optimum condensed sphere calculation for $\Omega_b = 1.0$, $f_v^{1/3} = 0.25$, and $R = 10^6$ are compared with the observed light-element abundance constraints on Figure 9. For the present purposes, we take the following conservative limits on the observed primordial abundances from Boesgaard and Steigman (1985): $Y_p = 0.239 \pm 0.015 \times 10^{-5} \leq$ D/H $\leq 2 \times 10^{-4}$; $1 \times 10^{-5} \leq {}^3$He/H $\leq 2 \times 10^{-5}$. For ^{7}Li, we take the results of the recent analysis of Mathews *et al.* (1989), which showed that due to the uncertainties of galactic chemical evolution and main-sequence destruction, together with a scarcity of data, the range of possible primordial ^{7}Li abundances which are consistent with observations could be as large as $10^{-10} \leq {}^7$Li/H $\leq 10^{-8}$.

Contrary to our previous results, the only light-element constraint which can be satisfied with $\Omega_b = 1.0$ is deuterium. As indicated by the box in Figure 9, this constraint is satisfied for a broad range of fluctuation separation radii, $r \sim 30$ to 3000 m. The other constraints are not satisfied even with these conservative limits and optimum conditions. The calculation does come tantalizingly close to the limits, however, for separation radii ~ 30–50 m.

To obtain a clearer picture of the possible limits on Ω_b for optimum inhomogeneous nucleosynthesis conditions we show

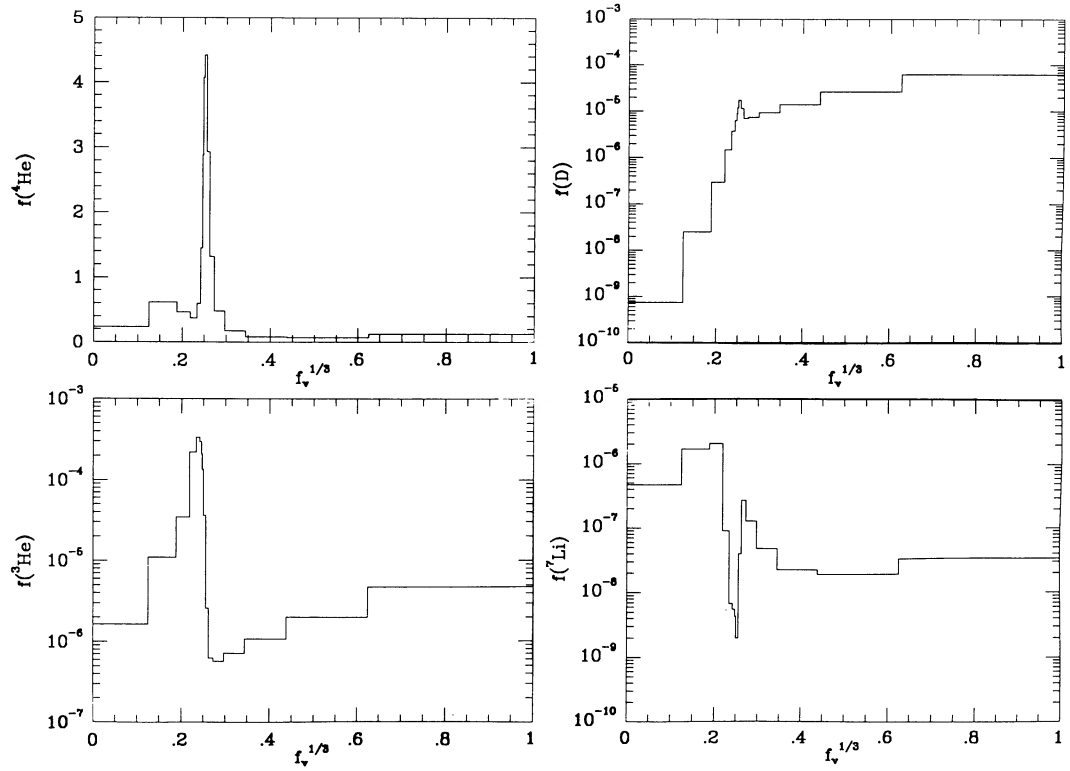

FIG. 8.—Nucleosynthesis contribution, $f = X_i \Omega_b \Delta f_v / \Delta f_v^{1/3}$, for different zones as a function of $f_v^{1/3}$

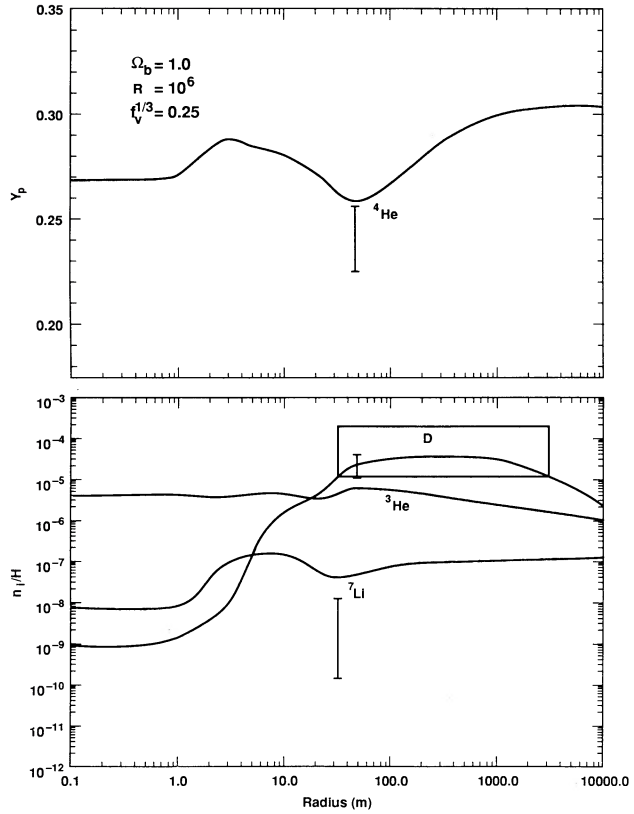

FIG. 9.—A best-fit $\Omega_b = 1.0$ inhomogeneous nucleosynthesis model with a spherical high-density fluctuation. Results are plotted as a function of separation radius, r.

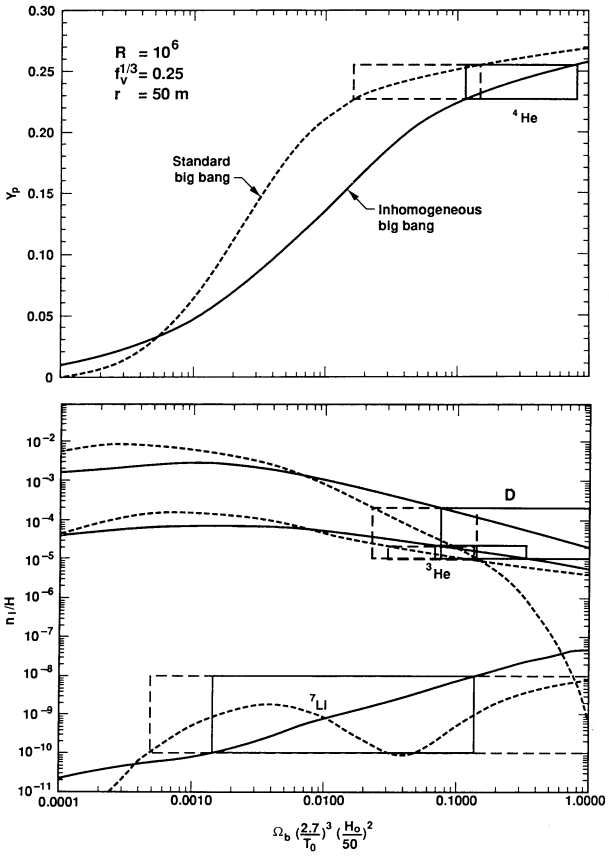

FIG. 10.—Calculated light-element abundance yields as a function of Ω_b. Solid lines are for an optimum inhomogeneous big bang with $R = 10^6, f_v^{1/3} = 0.25$, and $r = 50$ m and a spherical fluctuation shape. Dashed lines are for the standard homogeneous big bang. Boxes denote values consistent with the observed abundances of light elements.

in Figure 10 the calculated primordial abundances as a function of Ω_b for an inhomogeneous big bang with $R = 10^6$, $f_v^{1/3} = 0.25$, and $r = 50$ m. The values of Ω_b which are consistent with the adopted constraints are shown as boxes in this figure. Also shown for comparison are the results and limits from standard homogeneous big bang nucleosynthesis (*dashed lines*). From this figure, it is clear that although the standard big bang limits are $0.02 \leq \Omega_b \leq 0.15$ (primarily based upon the deuterium constraint), the limits based upon ^{4}He and deuterium in this particular inhomogeneous big bang model are $0.1 \leq \Omega_b \leq 0.8$. The ^{3}He constraint is somewhat more uncertain due to the production of ^{3}He in stars (see Boesgaard and Steigman 1985) and also due to the fact that the ^{3}He production does not depend very sensitively on Ω_b. However, from the adopted observed limits, we would place an upper limit of $\Omega_b \leq 0.4$ which is also consistent with the constraint derived if an upper limit of $Y_p \leq 0.24$ is adopted (Pagel and Simonson 1989; Torres, Peimbert, Peimbert and Fierro 1989). It has been pointed out (Yang *et al.* 1984) that a better constraint using ^{3}He is that of $(^3\text{He} + \text{D})/\text{H} \leq 10^{-4}$, since deuterium is converted to ^{3}He in stars. With this constraint, values of $\Omega_b > 0.2$ up to $\Omega_b > 1.0$ are consistent in this inhomogeneous big bang model. The ^{7}Li abundance constraint would be more restrictive (Kurki-Suonio *et al.* 1989). In this work, we would obtain a limit of $\Omega_b \leq 0.15$. However, the hydrodynamic expansion of the high–baryon-density regions during nucleosynthesis (Alcock *et al.* 1990) and/or an enhanced back-diffusion of neutrons (Malaney and Fowler 1988) is likely to cause a significant reduction of the synthesized ^{7}Li by the $^7\text{Li}(p,\alpha)^4\text{He}$ reaction. Hence, we prefer the more conservative upper limits to Ω_b based upon the helium and deuterium abundances alone.

V. CONCLUSION

We have computed light-element nucleosynthesis in baryon-number–inhomogeneous big bang models. The calculations utilized a multizone nucleosynthesis code in which the nuclear reaction network and baryon diffusion are solved together implicitly. We have parameterized the fluctuations as either spheres or spherical shells placed in a regular lattice of varying size. We find that within this simple parameterization there exist plausible fluctuation amplitudes, sizes, and separation distances for which most of the light-element abundance constraints can be satisfied (expect perhaps ^{7}Li) even for models with a much higher baryon density than that allowed by the standard homogeneous big bang. In particular, values of Ω_b as large as 0.8 may be possible. Our values for the upper limit to Ω_b are larger than that derived in Kurki-Suonio *et al.* (1990), primarily because we have considered the possibility of larger fluctuation amplitudes and a different geometrical shape (i.e., more compact) than in that work. It is clearly important to study the detailed physics of the QCD phase transition to see whether such fluctuation characteristics can emerge. In a forthcoming work, we will discuss this.

The authors gratefully acknowledge useful discussion with H. Kurki-Suonio, R. Matzner, L. McLerran, J. Potvin, and J. R. Wilson. Work performed under the auspices of the US Department of Energy by the Lawrence Livermore National Laboratory under contract number W-7405-ENG-48. We also acknowledge partial support from IGPP grant LLNL 90-08 and NSF grant PHY-8914379.

REFERENCES

Alcock, C. R., Dearborn, D. S. P., Fuller, G. M., Mathews, G. J., and Meyer, B. 1990, *Phys. Rev. Letters*, (in press).
Alcock, C. R., and Farhi, E. 1985, *Phys. Rev. D*, **32**, 1273.
Alcock, C. R., Fuller, G. M., and Mathews, G. J. 1987, *Ap. J.*, **320**, 439.
Alcock, C. R., Fuller, G. M., Mathews, G. J., and Meyer, B. 1989, *Nucl. Phys. A*, **498**, 301c.
Applegate, J. H., and Hogan, C. 1985, *Phys. Rev. D*, **30**, 3037.
Applegate, J. H., Hogan, C., and Scherrer, R. J. 1987, *Phys. Rev. D*, **35**, 1151.
———. 1988, *Ap. J.*, **329**, 572.
Audouze, J., Delbourgo-Salvador, P., Reeves, H., and Salati, P. 1988, in *Origin and Distribution of the Elements*, ed. G. J. Mathews (Singapore: World Scientific), pp. 86–96.
Boesgaard, A. M., and Steigman, G. 1985, *Ann. Rev. Astr. Ap.*, **23**, 319.
Dearborn, D. S., Schramm, D. Steigman, G., and Truran, J. 1989, *Ap. J.*, **347**, 455.
Frei, Z., and Patkos, A. 1989, *Phys. Letters*, **222B**, 469.
Fuller, G. M., Mathews, G. J., and Alcock, C. R. 1988, *Phys. Rev. D*, **37**, 1380.
———. 1989, in *Dark Matter*, ed. J. Audouze and J. Tran Thanh Van (Paris: Editions Frontiéres), pp. 303–318.
Gottlieb, S., Liu, W., Toussaint, D., Renken, R. L., and Sugar, R. L. 1987, *Phys. Rev. Letters*, **59**, 2247.
Kajino, T., Mathews, G. J., and Fuller, G. M. 1989, in *Heavy Ion Physics and Astrophysical Problems*, ed S. Kubono (Singapore: World Scientific), pp. 51–66.
Kurki-Suonio, H. 1988, *Phys. Rev. D*, **37**, 2104.
Kurki-Suonio, H., and Matzner, R. 1989, *Phys. Rev. D*, **39**, 1046 (KM89).
Kurki-Suonio, H., Matzner, R. A., Centrella, J. M., Rothman, T., and Wilson, J. R. 1988, *Phys. Rev. D.*, **38**, 1091.
Kurki-Suonio, H., Matzner, R. A., Olive, K. A., and Schramn, D. N. 1990, *Phys. Rev. D.*, in press.
Lee, T. D. 1987, *Phys. Rev. D*, **35**, 3637.
Malaney, R. A., and Butler, M. N. 1989, *Phys. Rev. Letters*, **62**, 117.
Malaney, R. A., and Fowler, W. A. 1988, *Ap. J.*, **333**, 14.
Mampe, W., Ageron, P., Bates, C., Pendlebury, J. M., and Steyeul, A. 1989, *Phys. Rev. Letters*, **63**, 593.
Mathews, G. J., Alcock, C. R., and Fuller, G. M. 1990, *Ap. J.*, **349**, 449.
Mathews, G. J., Fuller, G. M., Alcock, C. R., and Kajino, T. 1989, in *Dark Matter*, ed. J. Audouze and J. Tran Thanh Van (Paris: Editions Frontiéres), pp. 319–328.
Meyer, B., Alcock, C. R., Fuller, G. M., and Mathews, G. J. 1990, *Phys. Rev. D*, submitted
Pagel, B. E. J., and Simonson, E. A. 1989, *Rev Mexicana Astr. AF.*, **18**, 153.
Sumiyoshi, K., Kusaka, K., Kamio, T., and Kajino, T. 1989, *Phys. Letters*, **225B**, 10.
Terasawa, N., and Sato, K. 1989, *Phys. Rev.*, **D39**, 2893.
Torres-Peimbert, S., Peimbert, M., and Fierro, J. 1989, *Ap. J.*, **345**, 186.
Toussaint, D. 1989, private communication.
Witten, E. 1984, *Phys. Rev. D*, **30**, 272.
Yang, J., Turner, M. S., Steigman, G., Schramm, D. N., and Olive, K. 1984, *Ap. J.*, **281**, 493.

CHARLES R. ALCOCK and BRADLEY S. MEYER: Institute of Geophysics and Planetary Physics, Lawrence Livermore National Laboratory, P.O. Box 808, L-413, Livermore, CA 94550

GEORGE M. FULLER: Physics Department, B 019, University of California, San Diego, La Jolla, CA 92093

GRANT J. MATHEWS: Physics Department, Lawrence Livermore National Laboratory, P.O. Box 808, L-297, Livermore, CA 94550